



ELSEVIER

Materials Science and Engineering A319–321 (2001) 111–114

**MATERIALS
SCIENCE &
ENGINEERING****A**

www.elsevier.com/locate/msea

Ideal strengths of bcc metals

C.R. Krenn^{a,c,*}, D. Roundy^{b,c}, J.W. Morris Jr^{a,c}, Marvin L. Cohen^{b,c}^a Department of Materials Science and Engineering, University of California at Berkeley, Berkeley, CA 94720, USA^b Department of Physics, University of California at Berkeley, Berkeley, CA 94720, USA^c Materials Sciences Division, Lawrence Berkeley National Laboratory, Berkeley, CA 94720, USA

Abstract

We present ab initio ideal strength calculations in body-centered cubic (bcc) tungsten for ‘pencil-glide’ slip on {110}, {112}, and {123} planes and for the {100} cleavage strength. We use these results to analyze the tensile and shear strengths of other bcc metals. In all bcc metals, the minimum shear strength on any plane containing $\langle 111 \rangle$ is $\approx 0.11/S_{\langle 111 \rangle}$, where $S_{\langle 111 \rangle}$ is the elastic compliance for any shear in a $\langle 111 \rangle$ direction. The ideal cleavage strength on {100} for many bcc metals is $\approx 0.083/s_{11}$ where s_{11} is the single crystal elastic compliance. Comparison of the ideal shear and tensile strengths offers a measure of the inherent ductility or brittleness of a material. © 2001 Elsevier Science B.V. All rights reserved.

Keywords: Ideal strength; Bcc ductile–brittle transition; Pencil-glide

1. Introduction

Calculations of ideal strength are of great theoretical interest because they are an upper bound to the strength of any real crystal. Although they are computationally difficult, ab initio calculations are of particular interest because they offer quantitatively believable estimates of these upper bounds. With recent advances in computer technology, ab initio calculations of the ideal tensile strengths [1–3] and shear strengths [4,5] of body-centered cubic (bcc) metals are becoming more common.

We have recently completed a comprehensive ab initio study of the ideal strengths of tungsten for shear on each of the three common bcc slip systems and for a single axis of tension [6]. The shear systems examined were for the $\langle 111 \rangle$ directions on {110}, {112} and {123} planes. These systems are collectively described by the term ‘pencil-glide’. We only examined one direction of tension, $\langle 100 \rangle$, because prior theoretical and experimental work [3,7,8] all identify $\langle 100 \rangle$ axes as the weak directions in tension and {100} planes as the cleavage planes. This is a result of the geometry of the

Bain transformation, which produces the face-centered cubic (fcc) crystal structure after a small tensile deformation along $\langle 100 \rangle$.

Both the shear and tensile calculations allowed full structural relaxations orthogonal to the applied strains. These relaxations proved critical for identifying the simple crystallographic reason that the ideal shear strengths on all pencil-glide planes were nearly identical. In the present paper, we also discuss the implications of these calculations in tungsten for understanding the behavior of other bcc metals.

2. Ideal strength of bcc tungsten

The computational procedure is described fully in [6]. For each strained configuration of interest, the quasi-static ($T=0$) energy of the tungsten crystal and the Hellmann–Feynman stresses were calculated using the local density approximation (LDA) within a pseudopotential total-energy scheme incorporating semi-relativistic corrections [9,10]. The energy and stress were calculated as a function of strain under the functional equivalent of stress control. In this case, which provides the most meaningful measure of the ideal strength [11], the selected strain is fixed, and the other five independent strains are adjusted until their conjugate Hellmann–Feynman stresses are less than 0.15 GPa.

* Corresponding author. Tel.: +1-510-4866035; fax: +1-510-4864995.

E-mail address: crkrenn@lbl.gov (C.R. Krenn).

Fig. 1 shows the stress–strain behavior for tension along $\langle 100 \rangle$ and for shear on the three common slip systems of bcc. Also shown are sinusoidal fits to the stress–strain behavior. The agreement between the sinusoidal fits and the ab initio results is quite good. Even more striking is the close similarity of the stress–strain relations for $\langle 111 \rangle$ slip in the easy directions on the three planes. (The shear strengths on $\{112\}$ and $\{123\}$ planes are a function of the sign of the shear strain applied. We use the minimum-strength — or ‘easy’ — direction to define the ideal strength.)

The calculated shear strengths (18 GPa) are lower than the shear strengths inferred from nano-indentation experiments (26–28 GPa) [12]. However, the agreement is much better if a simple correction to the errors of linear-elastic Hertzian contact models is used to account for the deviations from linear-elastic response near elastic instability. With this correction, the experimental numbers drop to 16.5–18 GPa [6].

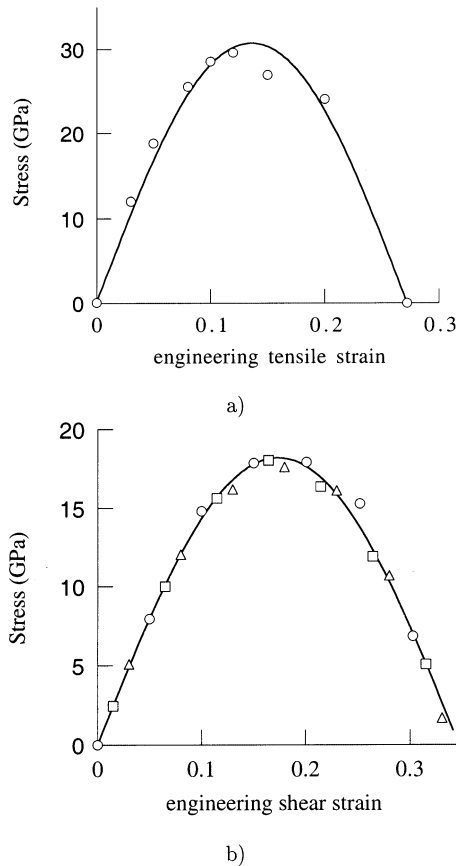


Fig. 1. Stress as a function of strain for tension along $\langle 100 \rangle$ and for $\langle 111 \rangle$ shear in the ‘easy’ direction on $\{110\}$ (\circ ’s), $\{112\}$ (\square ’s), and $\{123\}$ planes (\triangle ’s).

3. Source of the ideal strength

Two clear trends are apparent in the existing calculations of ideal strength [13]. First, the ideal strength in a particular deformation mode is proportional to the modulus that governs linear elastic deformation in that mode. Second, the constant of proportionality is fixed by the position of the nearest energetic extremum along the deformation path.

For $\langle 100 \rangle$ tension in bcc, the relevant relaxed modulus is given by

$$E_{\langle 100 \rangle}^r = \frac{1}{s_{11}} = \frac{(c_{11} - c_{12})(c_{11} + 2c_{12})}{c_{11} + c_{12}}, \quad (1)$$

where s_{ij} and c_{ij} are the single crystal elastic compliances and moduli. In all of the bcc transition metals, the nearest extrema along the tensile deformation path is a maximum corresponding to a fcc structure [1,14]. This is the Bain strain, $e_b = 0.26$, assuming a constant volume path for comparative purposes. In the bcc alkali metals, a nearer extrema is theoretically possible if the fcc phase is metastable instead of unstable.

There are two reasons for the nearly identical strengths on all the shear systems examined. First, the shear modulus for all three systems is identical. This identity is true for all bcc metals, and not just for tungsten, which happens to be elastically isotropic. Second, the position of the energetic extrema is also nearly identical for all three slip systems.

The modulus for shear will, in general, depend on both the shear direction and the shear plane, but, because of the 3-fold symmetry for rotation about $\langle 111 \rangle$ in bcc, any shear in a $\langle 111 \rangle$ direction has a relaxed modulus of

$$G_{\langle 111 \rangle}^r = \frac{1}{S_{\langle 111 \rangle}} = \frac{3c_{44}(c_{11} - c_{12})}{4c_{44} + c_{11} - c_{12}}. \quad (2)$$

The position of the energetic extrema also is nearly identical for all types of shear along $\langle 111 \rangle$ [6]. This is because of the relatively open structure of bcc, which has eight nearest neighbors at a distance of $0.866a_0$ and six next-nearest neighbors at a distance of a_0 , where a_0 is the lattice constant. An applied shear breaks the symmetry of these neighbors (Fig. 2). Again assuming constant volume deformation for comparative purposes, after a relaxed shear of 0.34, there is a high symmetry crossover point, which is identical for shear on $\{112\}$ or $\{123\}$ planes (Fig. 2b). Shear on planes with normals near $\langle 112 \rangle$ or $\langle 123 \rangle$ will also pass through this energetic maximum. A slightly different extrema geometry applies for shears on planes with normals close to $\langle 110 \rangle$ [6]. Both high symmetry extrema geometries are only reached if full atomic relaxation is allowed.

If we follow Frenkel [15] and Orowan [16] in assuming a sinusoidal form for the stress–strain curves, the

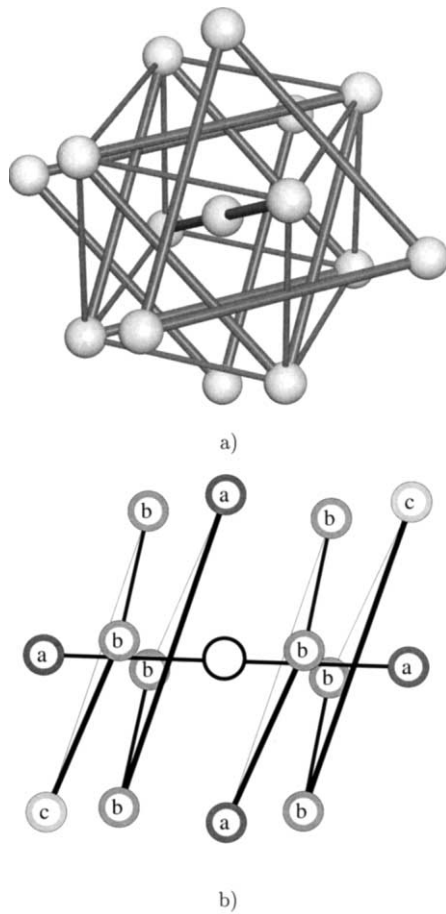


Fig. 2. Illustration of the symmetries of pencil-glide in bcc. (a) Illustrates the stacking sequence of the eight nearest and six next-nearest neighbors along the $\langle 111 \rangle$ direction in bcc. (b) Shows the symmetry of the $\{112\}$ and $\{123\}$ energetic extrema. In (b), the four a and eight b atoms each are at equal distances from the central atom.

stresses in tension (σ) and in shear (τ) will be a function of the tensile (ε) and shear (γ) strains:

$$\sigma = \sigma_{\langle 100 \rangle}^{\max} \sin \left[\frac{\pi \varepsilon}{0.26} \right] \quad (3)$$

and

$$\tau = \tau_{\langle 111 \rangle}^{\max} \sin \left[\frac{\pi \gamma}{0.34} \right], \quad (4)$$

where $\sigma_{\langle 100 \rangle}^{\max}$ and $\tau_{\langle 111 \rangle}^{\max}$ are the ideal strengths for tension and shear, respectively [13]. In the limit of small strain, $\sigma = E_{\langle 100 \rangle}^r \varepsilon$ and $\tau = G_{\langle 111 \rangle}^r \gamma$, and the ideal strengths are given by

$$\sigma_{\langle 100 \rangle}^{\max} \approx \frac{0.26 E_{\langle 100 \rangle}^r}{\pi} = 0.083 E_{\langle 100 \rangle}^r \quad (5)$$

and

$$\tau_{\langle 111 \rangle}^{\max} \approx \frac{0.34 G_{\langle 111 \rangle}^r}{\pi} = 0.11 G_{\langle 111 \rangle}^r. \quad (6)$$

The predictions of Eqs. (5) and (6) are quite close to the tungsten ab initio results of $0.072 E_{\langle 100 \rangle}^r$ and $0.11 G_{\langle 111 \rangle}^r$.

4. Discussion

Eq. (5) will give the ideal tensile strength of any bcc metal whose fcc structure is unstable. This is true in all the ab initio calculations of both Craievich et al. (Cr, V, Mo, Nb, W, Ta) [1] and those of Roundy and Cohen (Fe) [14]. It is not clear whether the bcc alkali metals will also have an unstable fcc phase. If they do not, and the sinusoidal fit to the stress–strain curve is still reasonable, Eq. (5) will overestimate the ideal tensile strengths.

Since any shear in a $\langle 111 \rangle$ direction in bcc has a relaxed modulus of $G_{\langle 111 \rangle}^r$ and because the period of the stress–strain curve for any $\langle 111 \rangle$ shear is ≈ 0.34 , the ideal shear strength of any pencil-glide system in any bcc metal will have an ideal strength given by Eq. (6). This is in marked contrast to the result of Frenkel that gives $\tau_{\max} = Gb/2\pi h$, where h is the interplanar spacing and b , the Burger's vector, is the length of the shortest lattice vector in the direction of slip [15,17].

Table 1 lists the elastic moduli and ideal strengths of all bcc metals as calculated from Eqs. (1), (2), (5) and (6). It also tabulates the ratio $\kappa = \tau_{\langle 111 \rangle}^{\max} / \sigma_{\langle 100 \rangle}^{\max}$. κ is a measure of the inherent ductility or brittleness of a material, and it can be defined in a given material by the ratio of the minimum shear strength in any slip system to the minimum tensile strength in any direction [17].

Although in most cases, bcc metals shear by dislocation motion, the ideal strength may be approached near grain boundaries and crack tips where dislocation motion is extremely difficult as the result of geometric pinning and dislocation pileups. In the limit of very small κ , a material will be inherently ductile. Any tensile load will produce yield by shear on a plane oriented roughly 45° to the tensile axis before a tensile instability (such as cleavage failure) is reached. This seems to be the case for fcc metals such as Cu, where κ is relatively small [18,19]. In the limit of large κ , a material will be inherently brittle. If such a material is loaded in simple shear, it will fail in a tensile mode on a plane oriented roughly 45° to the shear plane. We do note that even the most brittle materials, including diamond, can deform ductilely under the compressive constraint of an indenter.

For bcc materials, κ can be expressed as a function of the bulk modulus $K = (c_{11} + 2c_{12})/3$, the single-crystal Poisson's ratio $\nu' = (3K - 2c_{44})/(6K + 2c_{44})$, the anisotropy ratio $\Delta = (c_{11} - c_{12} - 2c_{44})/K$, and the critical strains $\varepsilon_{\langle 100 \rangle}^* = \varepsilon_b = 0.26$ and $\gamma_{\langle 111 \rangle}^* = 0.34$:

Table 1

Elastic moduli c_{ij} (from [20]), average Poisson's ratio ν , anisotropy factor Δ , relaxed tensile modulus $E_{\langle 100 \rangle}^r$, estimated tensile strength $\sigma_{\langle 100 \rangle}^{\max}$, relaxed shear modulus $G_{\langle 111 \rangle}^r$, estimated shear strength $\tau_{\langle 111 \rangle}^{\max}$, and the ratio $\kappa = \tau_{\langle 111 \rangle}^{\max} / \sigma_{\langle 100 \rangle}^{\max}$ for all bcc metals^a

| | c_{11} | c_{44} | c_{12} | ν | Δ | $E_{\langle 100 \rangle}^r$ | $\sigma_{\langle 100 \rangle}^{\max}$ | $G_{\langle 111 \rangle}^r$ | $\tau_{\langle 111 \rangle}^{\max}$ | κ |
|----|----------|----------|----------|-------|----------|-----------------------------|---------------------------------------|-----------------------------|-------------------------------------|----------|
| Li | 13.4 | 9.60 | 11.3 | 0.35 | −1.43 | 3.06 | 0.253 | 1.49 | 0.162 | 0.64 |
| Ba | 12.6 | 9.50 | 8.00 | 0.26 | −1.51 | 6.39 | 0.528 | 3.08 | 0.333 | 0.63 |
| Na | 7.59 | 4.30 | 6.33 | 0.36 | −1.09 | 1.83 | 0.152 | 0.880 | 0.0952 | 0.63 |
| K | 3.70 | 1.89 | 3.17 | 0.38 | −0.97 | 0.782 | 0.0647 | 0.375 | 0.0405 | 0.63 |
| Rb | 2.96 | 1.60 | 2.44 | 0.36 | −1.03 | 0.755 | 0.0625 | 0.361 | 0.0390 | 0.62 |
| Fe | 230 | 117 | 135 | 0.29 | −0.83 | 130 | 10.8 | 59.2 | 6.41 | 0.60 |
| Ta | 264 | 82.6 | 158 | 0.34 | −0.31 | 146 | 12.1 | 60.2 | 6.51 | 0.54 |
| W | 523 | 160 | 203 | 0.28 | 0.00 | 409 | 33.9 | 160 | 17.3 | 0.51 |
| Cr | 348 | 100 | 67.0 | 0.21 | 0.50 | 326 | 27.0 | 124 | 13.4 | 0.50 |
| Mo | 465 | 109 | 163 | 0.30 | 0.32 | 380 | 31.5 | 134 | 14.5 | 0.46 |
| V | 230 | 43.1 | 120 | 0.36 | 0.15 | 148 | 12.2 | 50.4 | 5.45 | 0.45 |
| Nb | 245 | 28.4 | 132 | 0.40 | 0.33 | 153 | 12.6 | 42.5 | 4.60 | 0.36 |

^a All moduli and strengths are in GPa; all other values are dimensionless.

$$\kappa = \frac{(1 - 2\nu')(9 + \Delta + \Delta\nu')}{2(1 + \nu')(9 + \Delta + (\Delta - 18)\nu')} \frac{\gamma_{111}^*}{\varepsilon_{100}^*} \quad (7)$$

This reduces to

$$\kappa = \frac{\gamma_{111}^*}{2(1 + \nu)\varepsilon_{100}^*} \quad (8)$$

when the material is isotropic, and so κ is inversely proportional to the average Poisson's ratio ν . Table 1 shows that bcc metals have intermediate values of κ , and suggest that they are conditionally ductile or brittle depending on the loading geometry. This is consistent with the ductile–brittle transition seen in most of the bcc transition metals. Finally, based on ideal strength arguments, this table suggests that Nb is the most ductile of all bcc metals.

Acknowledgements

This work was supported by the Director, Office of Energy Research, Office of Basic Energy Sciences, Materials Sciences Division of the US Department of Energy and by the National Science Foundation Grant No. DMR-9520554. Computational resources have been provided by the National Science Foundation at the National Center for Supercomputing Applications and by the National Energy Research Scientific Computing Center, which is supported by the Office of Energy Research of the US Department of Energy. All Department of Energy support was under Contract No. DE-AC03-76SF00098.

References

- [1] P.J. Craievich, M. Weinert, J.M. Sanchez, R.E. Watson, Phys. Rev. Lett. 72 (1994) 3076.
- [2] P. Alippi, P.M. Marcus, M. Scheffler, Phys. Rev. Lett. 78 (1997) 3892.
- [3] M. Šob, L.G. Wang, V. Vitek, Phil. Mag. B 78 (1998) 656.
- [4] P. Söderlind, J.A. Moriarty, Phys. Rev. B 57 (1998) 10340.
- [5] A.T. Paxton, P. Gumbsch, M. Methfessel, Phil. Mag. Lett. 63 (1991) 267.
- [6] D. Roundy, C.R. Krenn, M.L. Cohen, J.W. Morris, Jr., Phil. Mag. A (2001) in press.
- [7] F. Milstein, S. Chantasiriwan, Phys. Rev. B 58 (1998) 6006.
- [8] J.W. Morris, Jr., Z. Guo, C.R. Krenn, in: S. Midea, G. Pfaffmann (Eds.), Heat Treating: Including Steel Heat Treating in the New Millennium, An International Symposium in Honor of Professor George Krauss, ASM, Cincinnati, 2000.
- [9] J. Ihm, A. Zunger, M.L. Cohen, J. Phys. C 12 (1979) 4409.
- [10] M.L. Cohen, Phys. Scr. T1 (1982) 5.
- [11] J.W. Morris Jr, C.R. Krenn, Phil. Mag. A 80 (2000) 2827.
- [12] D.F. Bahr, D.E. Kramer, W.W. Gerberich, Acta Mater. 46 (1998) 3605.
- [13] J.W. Morris Jr, C.R. Krenn, D. Roundy, M.L. Cohen, in: P.E.A. Thrichi, A. Gonis (Eds.), Phase Transformations and Evolution in Materials, TMS, Nashville, 2000, p. 187.
- [14] D. Roundy, M.L. Cohen, Department of Physics, University of California, Berkeley, 1999, unpublished research.
- [15] J. Frenkel, Z. Phys. 37 (1926) 572.
- [16] E. Orowan, Rept. Prog. Phys. 12 (1949) 185.
- [17] A. Kelly, N.H. Macmillan, Strong Solids, third ed., Clarendon Press, Oxford, 1986.
- [18] M. Šob, L.G. Wang, V. Vitek, Kovové Materiály 36 (1998) 145.
- [19] D. Roundy, C.R. Krenn, M.L. Cohen, J.W. Morris Jr, Phys. Rev. Lett. 82 (1999) 2713.
- [20] D.F. Nelson (Ed.), Landolt-Börnstein LBIII/29a — Low Frequency Properties of Dielectric Crystals: Second and Higher Order Elastic Constants, Springer, Berlin, 1992.